Impact of Flow Regime on Polydispersity in Tubular RAFT Miniemulsion Polymerization

James P. Russum, Christopher W. Jones, and F. Joseph Schork
School of Chemical and Biomolecular Engineering, Georgia Institute of Technology, 311 Ferst Dr., Atlanta, GA 30332

DOI 10.1002/aic.10730
Published online February 22, 2006 in Wiley InterScience (www.interscience.wiley.com).

The flow characteristics of a miniemulsion in a tubular reactor were assessed using a modified dye tracer approach. Metered nitrogen was introduced producing isolated plug flow. The effects of the flow regime were then related to the polydispersity of polystyrene formed using reversible addition fragmentation chain transfer (RAFT). While nonideal flow was exhibited at very low Reynolds numbers ($\leq$ 20), laminar flow was not. This was attributed to fluid slippage at the wall of the reactor. It was demonstrated that the flow regime and residence time distribution have a direct effect on the molecular weight polydispersity of the polymer. Transient behavior during startup of isolated plug flow was attributed via experimental data and modeling to loss of initiator by way of water droplets left behind by the small cylinders of miniemulsion. © 2006 American Institute of Chemical Engineers *AIChE J,* 52: 1566-1576, 2006

Keywords: axial dispersion, controlled/living polymerization, miniemulsion, reversible addition fragmentation chain transfer (RAFT), tubular reactor

Introduction

The advent of controlled radical polymerizations[1] (CRP) has provided a potential means by which polymers of well-defined architecture can be synthesized using more forgiving and robust free-radical chemistry. In general, they utilize some reversible radical capping mechanism that limits the lifetime and, therefore, the probability of termination of the growing chains. While the nature of the mechanism varies, this reversible capping allows the chains to grow at the same rate with only small levels of termination, provided that the parameters of the recipe are suitably adjusted. To date, three techniques have garnered much of the attention of the research community, atom transfer radical polymerization (ATRP),[2, 3] nitroxide-mediated polymerization (NMP),[4] and reversible addition-fragmentation chain transfer (RAFT).[5, 6] Each of these techniques offers its own unique set of advantages and disadvantages. The best-behaved systems in terms of termination and polydispersity are the ATRP reactions, but the oftentimes large excess of metal complexes that are employed as the control agent are left in the polymer and have to be dealt with. The residual control agent is also an issue in polymers formed via NMP and RAFT, however, the compounds are not metal-based and the amounts necessary to control the polymerization tend to be less than all but the most active ATRP catalysts. Because the mechanism is similar, the benefits of NMP are akin to those of ATRP. At present, however, temperatures ($>$ 100°C) required to obtain reasonable reaction rates are an issue, as well as the small number of monomers that can be polymerized with a given nitroxide. Given this limitation, a number of current efforts are aimed at developing nitroxides that can mediate the reactions at temperatures below 100°C.[7, 8] Unlike NMP, RAFT can be employed at lower reaction temperatures and will polymerize a wide range of monomers and functionalities.[9, 10] While it suffers from an inherent termination dictated by the mechanism, this can be overcome in large part by keeping the molar ratio of RAFT agent to initiator sufficiently high. Because of its versatility, we consider it currently to be the most promising CRP technique for synthesizing polymers with well-defined architectures.

Correspondence concerning this article should be addressed to F. J. Schork at joseph.schork@chbe.gatech.edu or C. W. Jones at christopher.jones@chbe.gatech.edu.

Realizing that others have argued eloquently for the relaxation of the term "living", we have nonetheless chosen to employ "controlled" and not "living" to generally characterize these mechanisms. While they exhibit some living characteristics, for example, the ability of the chains to grow after the initial monomer charge is exhausted, our position is that they are different enough to warrant a distinction.

Aqueous dispersed systems are the dominant media used industrially for radical polymerizations, and, therefore, any CRP of commercial interest would likely need to be compatible with these media. Suspensions and emulsions are by far the most commonly employed commercial systems, but the aqueous system in which CRPs have been most successfully conducted to date is miniemulsion.[11-41] This is because of the predominant droplet nucleation in miniemulsions, as well as the fact that transport of the control agent across the aqueous phase is not required. To date, the overwhelming majority of published research of CRPs in miniemulsion has been directed at batch systems. Even so, continuous systems offer possibilities for polymer structure control that cannot be realized in batch systems. By combining stirred and tubular reactors in a train, one can in principle dictate the structure of the final copolymer. Such a reactor train could be used to design specific molecular structures to fit desired end-use properties. This allows the use of process design to carry out molecular design, or "product by process".

Our group has demonstrated the feasibility of employing RAFT in continuous miniemulsion reactors (both continuous stirred reactors and tubular reactors)[38-41] to make both homo- and copolymers. Enright[42] employed NMP/miniemulsion in a tubular reactor to make polystyrene. At present, there are no reports in the open literature of ATRP/miniemulsion in a continuous reactor, although Zhu[43, 44] have reported bulk ATRP in a continuous packed column. In this work, we expand on our earlier studies of styrene RAFT/miniemulsion polymerization in a continuous tubular reactor.[38, 40] The flow characteristics of the reactor are quantified utilizing a modified dye tracer technique developed exclusively for this type of heterogeneous system. Isolated plug flow was achieved using metered N_2, effectively producing an ideal flow regime. This allowed for the study of the effect of the residence time distribution (RTD) on the polydispersity (PDI) of the polymer produced. Finally, an unexpected transient behavior of the reactor during startup of isolated plug flow was observed and is explained using empirical data from solution experiments and a mathematical model.

Experimental

Materials

Styrene and butyl acrylate (monomers, ≥ 99.0%, Aldrich) were cleaned by either vacuum distillation or by passing through a column packed with inhibitor remover. The column packing was purchased from Aldrich and was specific to the type of inhibitor in the monomer. Potassium persulfate (initiator, KPS, ≥99.0 %, Aldrich), Triton X-405 (nonionic surfactant, TX405, 70% solution in water, Aldrich), hexadecane (co-stabilizer, ≥ 99.0%, Aldrich), and sodium dodecyl sulfate (ionic surfactant, SDS, ≥99%, Aldrich) were used as received. The RAFT agent, 1-phenylethyl phenyldithioacetate (PEPDTA) was synthesized following a procedure previously reported.[38, 45] The reagents for the RAFT agent synthesis, hydrochloric acid (37% in H_2O, Aldrich), magnesium sulfate (≥ 99%, Aldrich), *p*-toluenesulfonic acid (≥ 98%, Aldrich), benzyl chloride (≥ 99.9%, J.T. Baker), carbon disulfide (≥ 99.9%, J.T. Baker), carbon tetrachloride (≥ 99.9%, Aldrich), anhydrous diethyl ether (≥ 99.9%, Fisher),magnesium turnings (≥ 98.0%, Aldrich) and tert-butyl catechol (≥ 99%, Aldrich) were used as received. The oil-soluble dye, *N*-ethyl-*N*-(2-hydroxyethyl)-4-(4-nitrophenylazo)aniline (≥ 99.9%, Aldrich), was also used as received. Deionized water was generated in-house with a U.S. Filter Systems Deionizer and was used without further purification.

Table 1. Miniemulsion Recipe used in Tracer Study

Component	Mass, g	Basis
Water	50.0	
Styrene	50.0	100 wt-% of water
Triton X-405	0.58	~ 0.005 mol/L (in aqueous phase)
SDS	0.07	〃
Hexadecane	1.0	2 wt-% of monomer
Disperse Red 1	1.0	2 wt-% of monomer

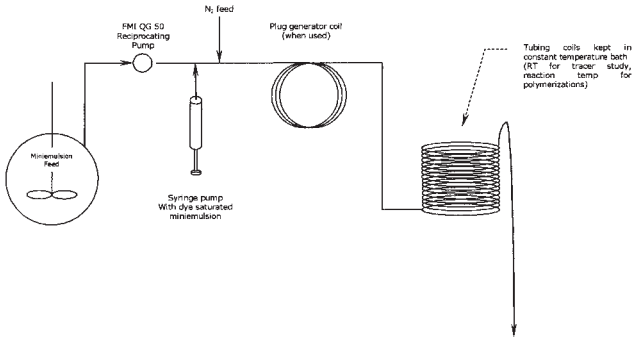

Figure 1. The tubular reactor utilized in this study.

Setup was used for tracer studies and polymerizations.

Miniemulsion preparation

The surfactants, SDS and TX405, were first added to water and allowed to mix for 15 min. The monomer, hexadecane, and RAFT agent were combined and allowed to mix for 15 min. The organic phase was then added to the aqueous phase and agitated vigorously with a magnetic stirrer for 30 min, forming a light yellow emulsion. The miniemulsion was formed by sonicating for 20 min (Fisher 300 Sonic Dismembrator at 70% output). During the sonication, the miniemulsion was cooled by an ice bath in order to keep the temperature low so that any thermal initiation of the monomer would be minimized.

Formation of dye saturated miniemulsion

The recipe for the dye saturated miniemulsion is shown in Table 1. The styrene was further inhibited by the addition of *tert*-butyl catechol to 0.5 wt-%. The dye was then dissolved in the styrene, followed by the addition of hexadecane. After mixing the surfactants in water, the aqueous and organic phases were sonicated (20 min, 70% output) together while agitated by a magnetic stirrer. During sonication the miniemulsion was cooled via ice bath.

Modified dye tracer experiments, isolated plug flow

The setup for conducting the modified tracer experiments is shown in Figure 1. The miniemulsion was fed into the reactor via an FMI QG 50 laboratory pump outfitted with a Kynar® pump head with carbon liner and ⅛-in. SS piston. The pump

was calibrated beforehand using deionized water and by measuring the time to fill a 5 mL volumetric flask at four different pump settings. A syringe pump was utilized to inject the dye-saturated miniemulsion into the reactor. All the tubing used was 1/8 in. OD – 1/16 in. ID PFA (perfluoroalkoxy, a copolymer of TFE). The reactor tubing was arrayed in helical coils (~25 cm in dia.) and submerged horizontally in a constant temperature, 75 L water bath. For all the dye experiments the bath was at room-temperature. For the isolated plug flow experiments, a coil used for plug generation (referred to hereafter as the plug generator) was included just before entering the reactor. This was incorporated because of the difficulty of maintaining a constant volume flow of nitrogen on a continuous basis. The length of the plug generator was 1/10 the length of the reactor. The feed was first started then the nitrogen was added to begin forming the isolated plugs. The nitrogen flow was metered by use of a needle valve located after the regulator on the nitrogen tank. After filling the plug generator to ~ ½ full, the dye saturated miniemulsion was injected by starting the syringe pump. When the generator was completely filled with plugs, the feed and syringe pumps were stopped. The feed pump was started again after all movement in the generator ceased. This allowed the determination of t_0 and τ by simply marking the reactor entrance and exit times of the first plug in the series. Samples were taken pre-determined intervals, noting that in this case since the length of the plug generator was $L_r/10$, the time frame for sampling was $\tau \pm \tau/20$.

Modified dye tracer experiments, simple tubular flow

In this instance, the plug generator coil was bypassed and no nitrogen was metered into the reactor, creating a constant, unbroken flow of miniemulsion. The dye-containing miniemulsion was injected at a known time and samples were subsequently taken at predetermined intervals. Since the Reynolds number was low enough to suggest laminar flow, ~ 10–20, the range of sampling was $\tau \pm \tau/2$.

Polymerizations in the tubular reactor

Polymerizations were conducted in a similar manner as the dye experiments, using the configuration shown in Figure 1 without the syringe pump. The reaction system was altered as mentioned in the prior section depending on whether or not isolated plug flow was desired. After preparing the miniemulsion, it was placed in the feed tank, and the requisite amount of initiator was added to the vessel. In order to suppress initiation before the feed entered the reactor, the feed vessel was kept at ~2 °C via submersion in a refrigerated water bath. Refrigeration and circulation were supplied by a VWR 1186D 28L programmable heating/cooling circulating bath. The feed was kept agitated via magnetic stirring and under ultra-high purity nitrogen throughout the experiment. For comparison to batch, feed samples were sealed in vials, purged with nitrogen, placed in the reactor water bath and polymerized for the requisite time.

The water bath was heated by a submersible heating coil and the temperature controlled with a thermocouple and temperature controller. Because of the high heat transfer inherent in tube reactors and the small size of the tubing in relation to the water bath, the temperature was assumed to be constant throughout the length of the submerged tubing. In order to insure that the inside of the tubing was completely dry before running the reaction, the reactor was filled with THF at room-temperature, pumped dry, heated to reaction temperature and purged with nitrogen overnight. The transparency of the tubing facilitated inspection for plugging and fouling.

Characterization

The samples from the tracer experiments were dried for 24 h in a vacuum oven (50 °C, ~ 100 kPa vacuum) and the residue was dissolved in 1 mL of THF. They were then analyzed using SEC/UV with the UV detector set at 503 nm. This is represents the absorption maximum of the dye and does not overlap with other system components. In this manner only the dye is seen in the UV. The areas under the UV peaks were determined and normalized for concentration using the area under the refractive index (proportional to total mass) peak of the polymeric surfactant, TX405.

After quenching with hydroquinone, polymer latex samples were dried in a consistent manner and monomer conversion was subsequently determined gravimetrically. Samples were dissolved in THF and run through a pipette column packed with alumina to remove the TX405 polymeric surfactant. The number-average molecular weight, M_n, and the polydispersity (PDI), M_w/M_n, were calculated using data gathered via size exclusion chromatography (SEC-Viscometry-RALLS) with THF as eluent. Three columns (American Polymer Standards styrene-divinylbenzene 100 Å, 1000 Å, and 10^5 Å) mounted in a Waters WAT038040 column heater set at 30°C were utilized. The columns were connected to a Viscotek GPCMax pump/autoinjector, a Viscotek T60A dual detector (viscometer and light scattering), a Waters 410 refractive index detector, an LDC Milton Roy Spectromonitor 3000 UV detector (at 254, 311, or 503 nm). Latex particle sizes and polydispersities were analyzed using quasi-elastic light scattering (QELS®, Protein Solutions DynaPro99 with DynaPro DCS v 5.26 software).

Results and Discussion

Modified tracer experiments

Traditionally, flow behavior in continuous reactors has been most often determined using dye or electrolyte injection techniques. The solute is injected, usually as either an impulse or step input, at some known time and the concentration is monitored at the outlet of the reactor. The concentration profile as a function of time reveals the flow characteristics of the reactor, and its deviation from nonideal flow. However, this classical method assumes a homogeneous reaction medium, a solution for example. Since miniemulsions are heterogeneous dispersions of droplets/particles in water, this technique requires modification in order to develop the correct flow profile for a given reactor. Since the polymerization takes place in the small, dispersed particles one needs information regarding their residence time, not that of the bulk fluid. This can be achieved in principle by simply adding an extremely hydrophobic dye to the monomer droplets. By injecting this dye-containing miniemulsion into the feed stream, a more accurate picture of the flow characteristics of the reactor during miniemulsion polymerizations is developed. In this work, and oil-soluble dye (*N*-ethyl-*N*-(2-hydroxyethyl)-4-(4-nitrophenylazo)aniline) was utilized. It was selected not only for its hydrophobicity, but also

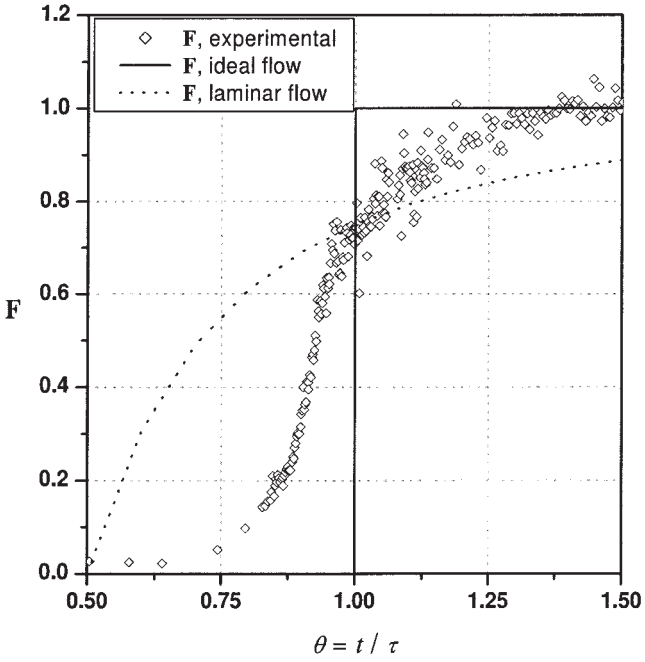

Figure 2. Experimental and theoretical step response curves for miniemulsion in tube reactor, $R_e \sim 20$.

for its maximum or peak absorbance, $\lambda_{max} \sim 503$ nm. This is much higher than the absorbance of any of the system components and important because the UV response of the effluent should only derive from the dye for the results to be useful. This was confirmed by SEC/UV of the UV active system components, styrene and TX405. Figure 2 shows the results of the tracer experiment. The dotted line represents the theoretical **F**-curve for a tubular reactor in laminar flow

$$\mathbf{F} = 1 - \frac{1}{4\theta^2} \text{ for } \theta \geq \frac{1}{2} \text{ where } \theta = t/\tau \tag{1}$$

The data reveal that the flow profile in the reactor deviates from the ideal. The degree to which a given flow exhibits nonideal behavior is frequently quantified by use of the dispersion model,[46] an analog to Fick's law of diffusion in a cylinder. In dimensionless form it is represented by

$$\frac{\partial C}{\partial \theta} = \left(\frac{\mathbf{D}}{uL}\right)\frac{\partial^2 C}{\partial \zeta^2} - \frac{\partial C}{\partial \zeta} \tag{2}$$

where

$$\zeta = (ut + z)/L \text{ and } \theta = t/\tau = tu/L$$

and the dimensionless group $\mathbf{D}/uL$ is called the vessel dispersion number. It is this parameter that is commonly used as a measure of the degree axial dispersion in a tubular reactor. As $\mathbf{D}/uL$ approaches zero, the flow profile approaches ideal. Conversely, as $\mathbf{D}/uL$ increases, the flow profile becomes less ideal, approaching mixed flow. At the extremes:

$$\frac{\mathbf{D}}{uL} \rightarrow 0 \text{ ideal (plug) flow}$$

$$\frac{\mathbf{D}}{uL} \rightarrow \infty \text{ mixed flow}$$

Provided deviations from ideal are small, the RTD curve is symmetric and analytic solutions are available to Eq. 2, allowing easy determination of $\mathbf{D}/uL$ from the tracer curve. For larger deviations, when the RTD curve is nonsymmetrical, analytic expressions are not available and numerical methods must be used to calculate $\mathbf{D}/uL$. A close examination of the data presented in Figure 2 reveals that in this case the step response is nonsymmetrical, indicating a large deviation from ideal. In order to quantify the degree of nonideality and the vessel dispersion number, the step response curve must first be converted to a pulse response curve. They are related by

$$\frac{d\mathbf{F}}{dt} = \mathbf{E} \tag{3}$$

where **E** represents the pulse response curve. Here, the data are fitted using a smoothing spline,[47] then differentiated numerically using a central difference formula to yield the necessary RTD curve, shown in Figure 3 . As a point of reference, curves representing small and large deviations from ideal flow are shown. The nonideality of the flow profile in the reactor is apparent when comparing the response curve generated from the data to that for near ideal flow. The reactor curve is clearly nonsymmetrical and skewed to the left, as would be expected

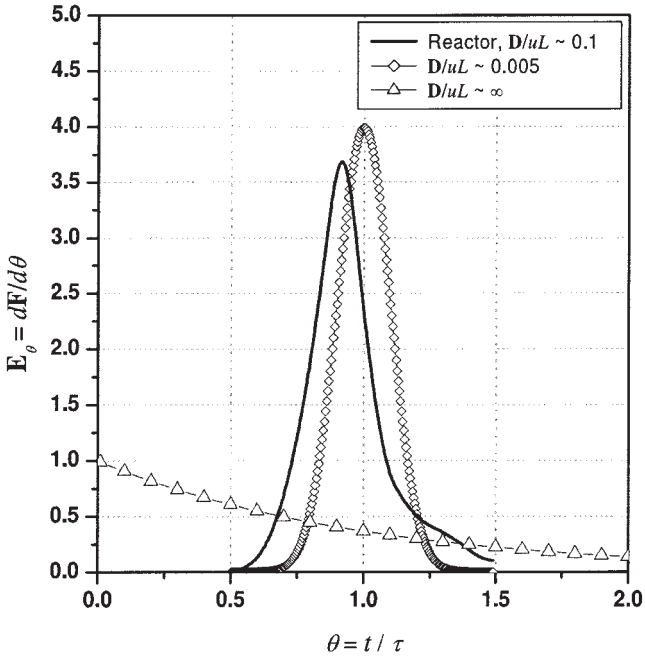

Figure 3. Pulse response curve (E_θ curve) calculated from step response data.

The two other curves compare the actual flow profile to curves that represent very small deviation from ideal flow ($\mathbf{D}/uL \sim 0.005$) and mixed flow ($\mathbf{D}/uL \sim \infty$).

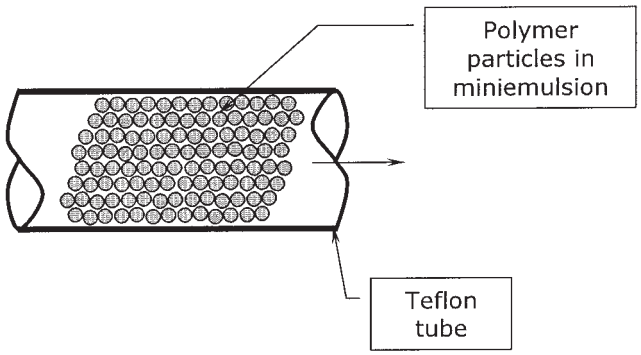

Figure 4. Miniemulsion flowing through tube with slippage at the tube wall.

as the flow deviates from ideal and approaches mixed flow. The extent of the deviation can be determined by examining the variance of the curve using the following expression which requires no assumptions about the magnitude of the dispersion number

$$\sigma_\theta^2 = 2\left(\frac{\mathbf{D}}{uL}\right) - 2\left(\frac{\mathbf{D}}{uL}\right)^2 [1 - e^{-uL/\mathbf{D}}] \tag{4}$$

It should be noted that this expression was derived utilizing closed boundary conditions. This "closed vessel" model is employed based on the experimental conditions where the flow pattern is expected to change at the point of injection, as well as at the outlet of the tube where the samples were collected. The vessel dispersion number was calculated to be ~ 0.10, an order of magnitude larger than what is normally considered to represent a small deviation ($\mathbf{D}/uL < 0.01$).[46]

The flow regime is not laminar. Considering the low Reynolds number ($\sim$20), this result is unanticipated. It can be explained in part by noting that in order to have fully developed laminar flow, a no-slip condition is required at the wall of the tube. In this case, the use of PFA tubing in combination with an aqueous dispersed system contributes to considerable slippage at the wall (see Figure 4). The surface tension of the aqueous phase is too high for the water to wet the wall of the PFA tube to any large degree. This conclusion is based also upon the physical observation that isolated plugs of miniemulsion flowing through the reactor did so without the considerable tailing that would be characteristic of no-slip conditions. This absence of tailing was observed in both the room-temperature dye experiments and the reaction temperature polymerizations. This suggests that at the higher reaction temperatures, decreased interfacial tension between the aqueous phase and the wall of the tubing (that is, better wetting and adhesion) was not significant enough to induce laminar flow. The fact that the flow profile is nonideal suggests that diffusive effects arising from the ability of the each individual droplet/particle to move freely through the aqueous phase are primarily responsible for the observed RTD. In other words, in the absence of no-slip conditions there would be little or no velocity profile. However, diffusive effects could still impart a residence-time distribution and that is the governing factor here. One other point should be highlighted for reasons that will become apparent in the forthcoming discussion of the polymerizations. When viewed on a physical length scale, the dispersion here is quite broad. The first traces of dye begin to show up at roughly $\tau - 0.37\tau$ and level off around $\tau + 0.37\tau$. In terms of length, the range of the dispersion is $2 \times 0.37\ L_r$, or $\sim$ 4500 cm.

One laboratory technique that is used to induce ideal flow without the high flow rates normally required is the introduction of an inert gas, for example, nitrogen, into the fluid flow.[49,50] If metered properly, the fluid will separate into individual elements, small cylinders or "plugs" (See Figure 5). Provided that the plugs are short compared to the length of the reactor, axial dispersion is minimized and, in principle at least, flow profiles approaching ideal flow can be achieved. This regime is referred to in this work as isolated plug flow so as to avoid confusion with what is classically known as plug flow. In order to insure the assumption of ideal flow, a tracer experiment was performed on these isolated plugs. The results are shown in Figure 6, and compared to both ideal and laminar flow. While the data reveal some deviation, on the whole they demonstrate that for this system the assumption of ideality holds.

Polymerizations

In order to assess the influence of the flow regime on the PDI of the polymer, polymerizations of styrene were conducted in the two flow regimes previously discussed. The results are summarized in Table 3. As expected with nonideal flow, the PDI of the polymer formed is higher than that synthesized in batch. In each of runs T1-T4 the PDI is significantly higher (5.4 – 7.7%) than the corresponding batch runs, B1–B4. Provided all else is equal, this would be attributable to the residence-time distribution imparted to the droplet/particles as they flow through the reactor. In a conventional free-radical polymerization, the lifetime of a growing chain is relatively short, on the order of one second. As such, residence time distributions have little effect on PDIs. In a controlled polymerization, however, the lifetime of a growing chain can approach its residence time in the reactor. To achieve a narrow PDI, the chains must all initiate quickly and grow at the same rate for the same amount of time. With a residence-time distribution, this cannot occur. The degree of the flow nonideality will dictate the degree to which the PDI is affected. It follows that in the limit of ideal flow, where there is no residence-time distribution, the PDI of

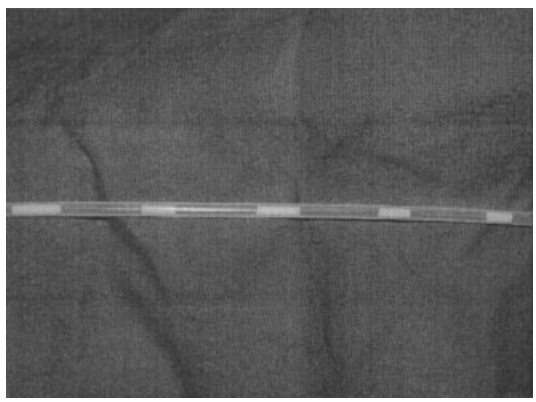

Figure 5. Miniemulsion using metered nitrogen to induce isolated plug flow.

In this instance, the length of the "plugs" moving through the reactor tubing is $\sim$1 cm.

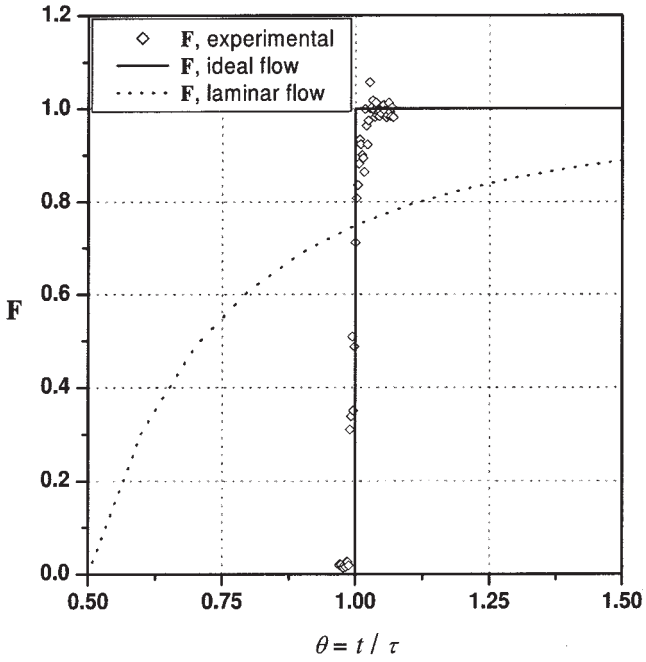

Figure 6. Experimental and theoretical step response curves of miniemulsion in isolated plug flow.

the polymer will be identical to that formed in a batch reactor. Runs T5–T7 and B5-B7 compare polymer formed in batch to polymer formed in the tubular reactor via segregated plugs. The PDIs of the polymers formed are much closer, and the case of T5/B5, the PDI of the polymer formed in the tube was slightly lower than that formed in the batch reactor.

One interesting finding that was unexpected was the transient behavior of the tube reactor while in isolated plug flow. Given a stream of equally spaced and completely isolated small plugs of reactant flowing through the reactor, one expects that if they all have the same residence time that each plug will exit the reactor with the same conversion. Each plug would behave as a batch reactor, and its average residence time in the reactor would be equivalent to time in a batch reactor. In other words, there would be no transient behavior because there is no steady state to be reached. In this case, something different was observed in practice. Figure 7 shows the results of three different polymerizations conducted at three different residence times. In each case the miniemulsion was in isolated plug flow using metered N_2. The arrows indicate the general trend in conversion as the plugs exited the reactor. The first plugs out were always at much lower conversions than batch and the

Table 2. Recipe for the Miniemulsion Polymerization of Styrene in Tubular Reactor

Component	Mass, g	Basis
Water	80 g	
Styrene	20 g	25 wt-% of water
Triton X-405	0.1 g	~ 0.005 mol/L (based on aqueous phase)
SDS	0.9 g	"
Hexadecane	0.4 g	2 wt-% of monomer
PEPDTA	0.1 g	$[Sty]_0/[PEPDTA]_0 = 500$
KPS	0.10 g	$[PEPDTA]_0/[KPS]_0 = 1$
Temperature	70 °C	

Table 3. Comparison of Batch and Tube Number Average Molecular Weights and PDIs

Run	Flow Regime	Conversion	M_n, theo	M_n, actual	M_w/M_n	Δ%
T1	Simple	57%	30388	28056	1.37	5.4
B1	—	57%	30468	30299	1.30	
T2	Simple	58%	30621	28839	1.38	7.0
B2	—	58%	30590	29731	1.29	
T3	Simple	91%	48283	45056	1.35	7.1
B3	—	92%	48774	48068	1.26	
T4	Simple	92%	48921	46398	1.40	7.7
B4	—	93%	49002	48435	1.30	
T5	Isolated plug	22%	11526	11846	1.38	−2.1
B5	—	24%	10389	12786	1.41	
T6	Isolated plug	52%	26251	26800	1.66	0.6
B6	—	52%	26694	27725	1.65	
T7	Isolated plug	89%	45433	46081	1.26	4.1
B7	—	91%	46359	44995	1.21	

conversion increased as a function of time (elapsed time, t, not residence time, τ). In order to assess this behavior, more complete sets of data were collected and are shown in Figure 8. In these two experiments, samples were taken starting at $t + \tau$ at time intervals of $\Delta t \sim \tau/100$ until the charge in the plug generator was exhausted ($\sim\tau/10$). The dotted lines represent the ideal, or batch, conversion for the residence time employed. Those ideal conversions were determined from concurrent batch experiments and are presented as a reference point. What they show is a reactor exhibiting transient start-up behavior, where conversions start out much lower than predicted, increase over time and eventually reach a steady state at batch conversions. It was thought initially that residual dye in the tubing may have some affect on the reaction. However, after

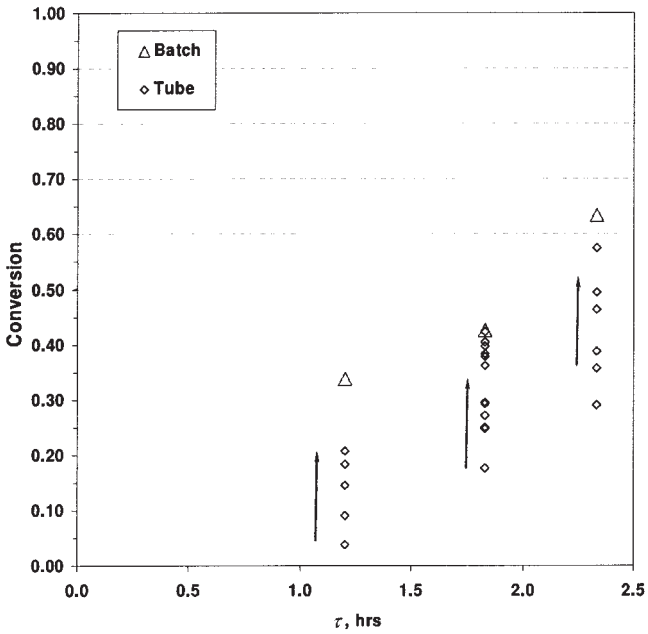

Figure 7. Conversion vs. average residence time, tube and batch samples.

Tube reactor in isolated plug flow (~1 cm plug miniemulsion, ~2 cm N_2). Arrows indicate tube samples taken as time progressed, conversion in the tube starts lower than batch and gradually increases.

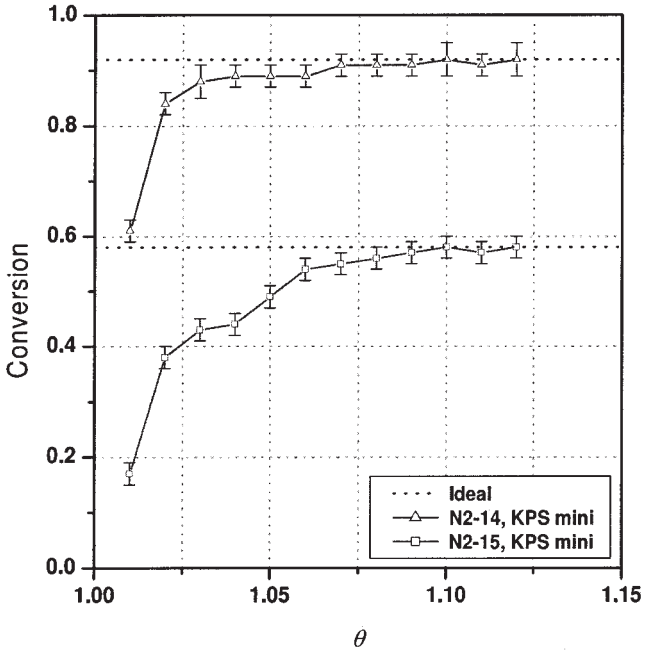

Figure 8. Conversion profile in tube reactor using miniemulsion in isolated plug flow (~1 cm plug miniemulsion, ~2 cm N_2).

Last two data points in each series had no N_2, that is, no plugs. ($\Theta = t/\tau$.).

replacing all of the tubing, the behavior persisted. A common practice that might otherwise account for such behavior is to start the reactor with the tubes full of water, but in this case extreme care was exercised in order to ensure that every component of the system (tube, pumps, fittings, and so on) was completely clean and dry before starting. Additionally, the entire system was purged with N_2 for several hours beforehand to prevent any effect on the polymerization from oxygen contamination. Assuming that the system is neither diluted nor contaminated, then two observations can be made about the data. First, in view of the nature of the system one might imagine that given the surface to volume ratio of the small plugs (~2 cm^{-1} for a 1 cm plug) some surface effect might be occurring that contributes to slower kinetics. However, if that alone were the cause then the conversion would be expected to remain at depressed levels. Each plug would exhibit similar kinetics regardless of when it entered and exited the reactor. In other words, in the complete absence of other effects, if something were happening independently in each individual plug then the conversion profile should be flat, but at a lower level than batch. This points toward the second hypothesis, that given the nature of the transient behavior, the plugs must be interacting in some manner.

In light of this supposition, an observation made during the polymerizations and initially thought to be inconsequential becomes important. It was noted that occasionally very small droplets were left behind by the plugs as they moved through the reactor. Since the droplets appeared transparent, they would likely be composed primarily of water and dissolved KPS, containing only relatively small numbers of particles. If that were the case then it is possible that the miniemulsion plugs were being "stripped" of water and initiator as they traversed the length of the tube. If significant, it might explain the transient behavior. As later plugs pick up the stripped initiator left behind by the earlier plugs, the effect would be the most pronounced on the first plugs through. The system would come to some steady-state level after a sufficient number of plugs traversed the reactor.

To test the basic hypothesis, two experiments were conducted at different average residence times using solution polymerization instead of miniemulsion. Since the solution system is homogeneous, the small droplets left behind would have the same composition as the larger plugs. However, because the droplets remain stationary while the plugs continue to move, their residence time would be slightly longer than the plugs they would encounter. This would tend to increase the overall conversion as compared to batch at the same average residence time. In this case, the effect would be different from the miniemulsion case. The first plugs out should be at the same conversion as batch because they have had few or no droplet encounters. The conversion would increase from this point to some steady state level. The results, which are shown in Figure 9 give support to the droplet theory. Again, the samples were taken starting at $t + \tau$ at time intervals of $\Delta t \sim \tau/100$ until the charge in the plug generator was exhausted ($\sim\tau/10$). The conversion of the first plugs out is almost identical to batch at the same average residence time and the conversion increases slowly from then on as time passes. The last two data points before the end of each run were from samples taken in the normal flow regime, that is, without the use of metered N_2. In other words, the nitrogen flow was stopped, eliminating the formation of plugs. The data show that the conversion quickly drops to that predicted by the average residence time of the solution.

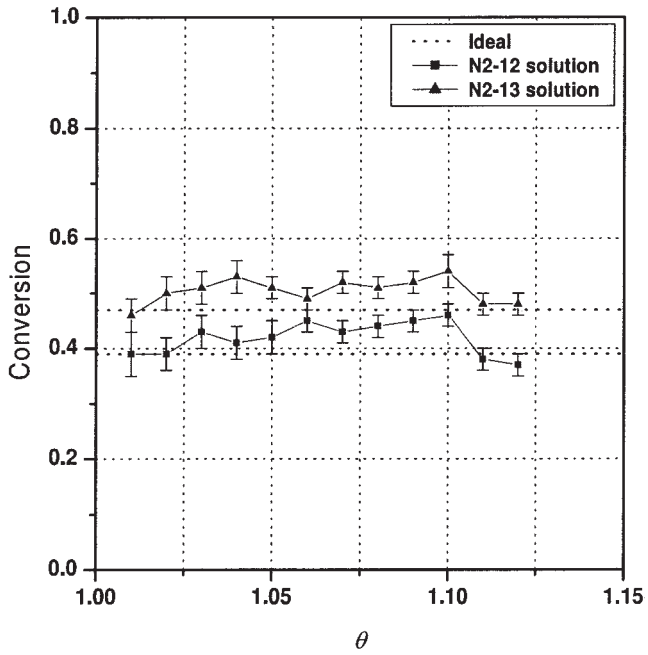

Figure 9. Conversion profile in tube reactor using solution polymerization in isolated plug flow (~1 cm plug solution, ~2 cm N_2).

Last two data points in each series had no N_2, that is, no plugs.

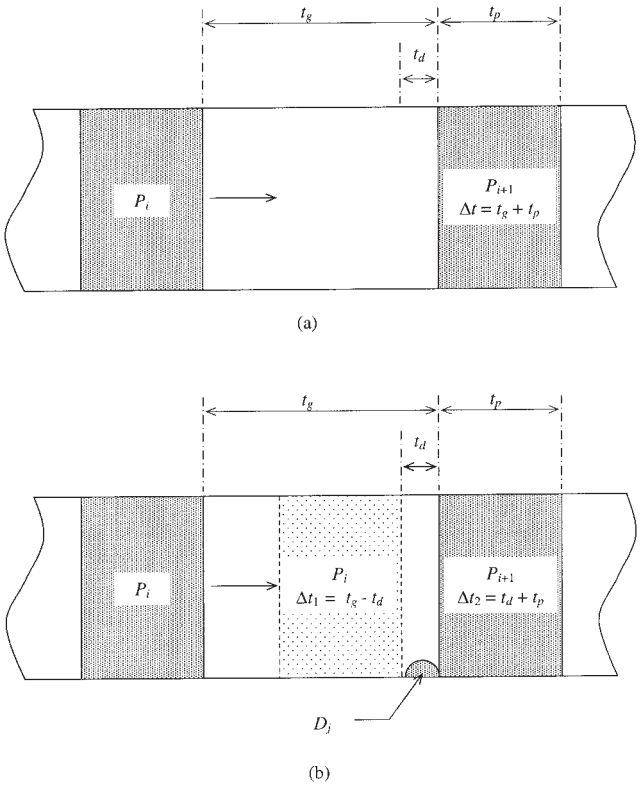

Scheme 1

In an effort to further scrutinize the theory, a model of the initiator concentration and monomer conversion at the outlet of the reactor was developed. Scheme 1 shows the form and basic notations for model development. If no droplets are present, then the system is represented by Scheme 1a where $\Delta t = t_g + t_p$ and

$$\frac{dI_i^P}{dt} = -k_d I_i^P \tag{5}$$

The defining event, Scheme 1b, occurs after plug P_i travels $\Delta t = t_g - t_d$ across the gap between it and the preceding plug, P_{i+1}, at which point it encounters droplet, D_j. During $\Delta t = t_d + t_p$, P_i incorporates and releases D_j. For all plugs except the first plug through the reactor this event can be represented mathematically by

$$V_i^P \frac{dI_i^P}{dt} = q_D I_j^D - q_D I_i^P - V_i^P k_d I_i^P \tag{6}$$

One simplification is the assumption that the plug volume remains constant at V_0 for all but the first plug through the reactor. For the first plug through the reactor, recognizing that the volume would change with each droplet it releases

$$V_1^P \frac{dI_1^P}{dt} = -q_D I_1^P - V_1^P k_d I_1^P \tag{7}$$

where

$$V_1^P = V_0 - jV_D \tag{7a}$$

Finally, for the droplets during the time $\Delta t = t_g - t_d$:.

$$\frac{dI_j^D}{dt} = -k_d I_j^D \tag{8}$$

All conversion occurs in the plugs and is represented by

$$\frac{dX_i}{dt} = k_p(1 - X_i)\left(\frac{2fk_d I_i^P}{k_t}\right)^{1/2} \tag{9}$$

This assumes conventional free radical first-order kinetics where chain transfer is not taken into account. For P_1, when there is no droplet release Eqs. 5 and 9 are integrated across $\Delta t = t_g + t_p$. When P_1 releases, Eqs. 5 and 9 are first integrated across $\Delta t = t_g - t_d$, followed by integrating Eqs.7 and 9 across $\Delta t = t_d + t_p$. The concentration of D_j is set at , and the volume is incremented down via Eq. 7a and substituted back into Eq. 7 during the next P_1 droplet release. For plugs P_2 to P_n a similar calculation is carried out using Eqs. 5, 6, 8, and 9 noting that now the plug volume remains constant at V_0. If there is no droplet encounter, the plug is integrated across $\Delta t = t_g + t_p$ and incremented to I_{i+1}^P and X_{i+1}, respectively. For droplet encounters, the plug and droplet are both integrated across $\Delta t = t_g - t_d$ using Eqs. 5, 8 and 9. Next, they are integrated using Eqs. 6 and 9 across $\Delta t = t_d + t_p$ after which the plug is incremented to to I_{i+1}^P and X_{i+1} and I_j^D is set to I_{i+1}^P. For each plug that traverses the reactor the process is repeated $\tau/(t_g + t_p)$ times. The parameters used in the model are shown in Table 4 and reflect the actual lengths, tube inner diameter and average velocity employed in one of the original experiments. In constructing the model, the droplet volumes are also assumed constant and of the same volume and size regardless of the volume of the plug that released it. The droplet volume V_d was estimated based on observation of the actual droplets and was held constant at $V_{p,1}/100$ where $V_{p,1}$ is the volume of a plug 1 cm in length. They are modeled to be a hemisphere so that t_d is constant and simply a function of the diameter of the sphere that would be formed from two droplets. The model also assumes that the droplets are formed only by releases from the first plug through and that no new droplets are created (or existing droplets disappear) afterward. This assumption is based on observing the be-

Table 4. Model Parameters

Quantity	Value	Units
L_r	6000	cm
L_p	1	cm
L_g	2	cm
u	0.4	$cm \cdot s^{-1}$
k_d	2.2×10^{-5}	s^{-1}
k_p	475	$L \cdot mol^{-1} \cdot s^{-1}$
k_t	6.1×10^7	$L \cdot mol^{-1} \cdot s^{-1}$
d_i	0.1651	cm
V_d	$V_{p,1}/100$	cm^3
$V_{p,1}$	$\pi/4 \cdot d_i^2 \cdot 1$ cm	cm^3
n_p/n_d	25	
f	0.65	

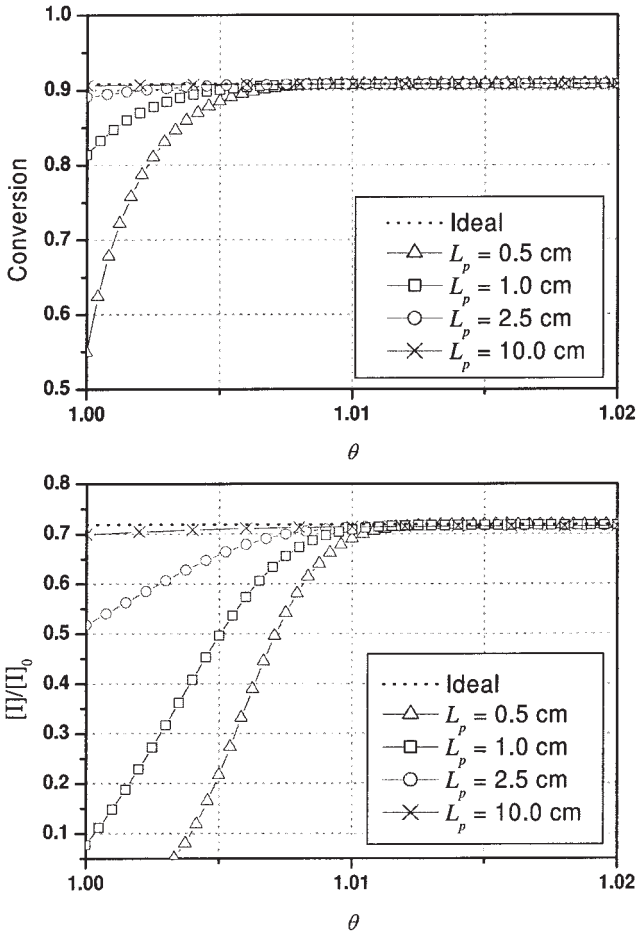

Figure 10. Evolution of outlet initiator concentration and conversion with dimensionless residence time in isolated plug flow in a tubular reactor.

Results shown at four different plug lengths.

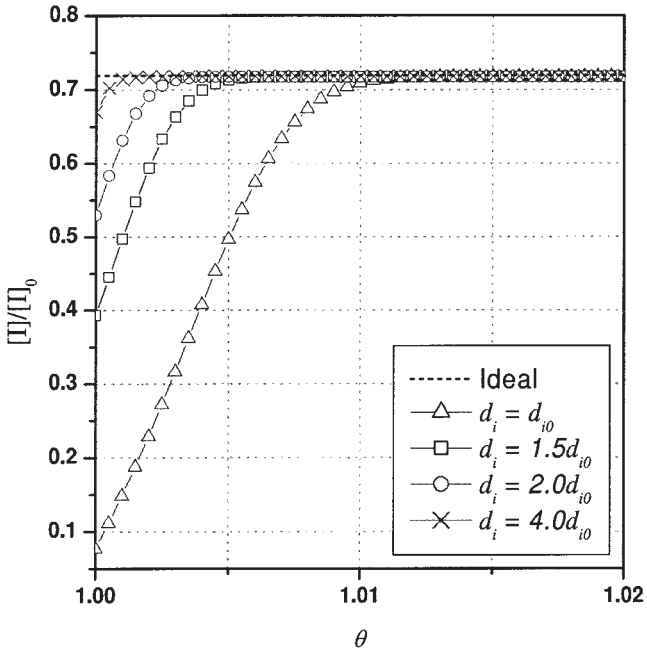

Figure 11. Effect of tube diameter on the outlet initiator concentration in isolated plug flow in a tubular reactor.

Results shown at four different tube diameters.

havior of the actual droplets in the reactor. The term n_p/n_d is the ratio of the total number of plugs to the total number of droplets, and was also estimated based on observation.

Figure 10 shows the results produced by the model at 4 different plugs lengths. The results show that both the initiator concentration and the overall conversion are adversely affected as the length of the plug decreases, behavior similar to that observed experimentally. Increasing the plug length, and, therefore, the plug volume, very quickly reduces the transient behavior. At plug lengths of 10 cm, the behavior is almost eliminated. A similar trend occurs by increasing the diameter of the tubing, as shown in Figure 11. This may explain in part why this phenomenon has not been reported in past studies using isolated plug flow. In the work of Poehlein,[49, 50] the tubing size was at least twice that used in this study. It also has important implications for future work that might include utilizing even smaller tube diameters. It should be also be noted that in commercial systems of large diameter, these effects would become insignificant. In fact, classic plug flow could be expected.

Using these insights, by increasing the length of the plugs in the actual reactor the transient behavior was essentially eliminated. The results of three different polymerizations are shown in Figure 12. In this case, the plug length was increased to ~ 20 cm. The data show that the conversion in the tube is similar to that in batch from $t = \tau$ onward. While some scatter exists, there is no drift in the conversion as is seen in Figure 7. The

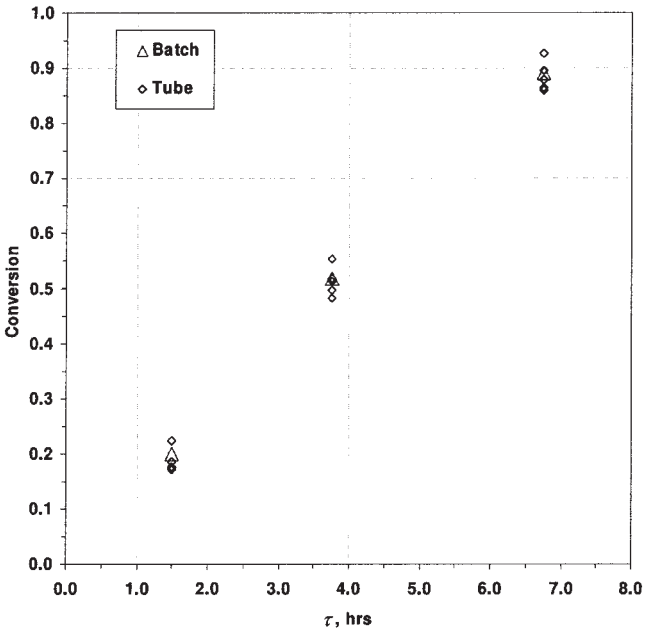

Figure 12. Conversion vs. average residence time, tube and batch reactions.

Tube samples taken over time, starting with first plugs out. Tube and batch conversions are similar with no transient conversion drift. Plug size ~20 cm.

first plugs out are at similar conversions to batch and the conversion remains at that level as the following plugs exit the reactor.

Conclusions

In this work, the flow characteristics of a tubular reactor were determined using a modified dye tracer approach. It was shown that by utilizing an oil-soluble dye, the droplet/particle flow behavior of a miniemulsion could be quantified. Dye tests performed in normal flow at low Reynolds numbers revealed that the reactor was not operating in laminar flow, and that the axial dispersion was quite high. The vessel dispersion number was calculated to be ~ 0.1. RAFT polymerizations conducted in this regime were compared to batch and the polymer formed was shown to have higher PDIs than polymer formed in batch. Dye tests carried out in isolated plug flow demonstrated the near-ideal nature of the flow regime. Polymer formed by RAFT polymerizations in this regime was shown to have similar PDIs as that formed in batch. Taken together this establishes a direct relationship between the residence time distribution and final polydispersity of the polymer formed in a controlled radical polymerization. Finally, transient behavior in isolated plug flow was demonstrated to be caused by loss of water and initiator by the plugs as they traversed the reactor. It was further shown that the effects could be minimized by either increasing the plug length or the tube diameter.

Acknowledgments

The authors would like to thank the National Science Foundation for funding this work (CTS-0234658).

Notation

μ = absolute viscosity, P
ρ = density, gm $\cdot$ cm^{-3}
σ_θ = variance of $\mathbf{E}_\theta$ curve, dimensionless
τ = average residence time in reactor, s
θ = dimensionless residence time, t/τ
$\boldsymbol{D}$ = diffusion coefficient, cm^2 $\cdot$ s
D_j = droplet j
d_i = inner diameter of tube, cm; $d_{i,O}$, initial inner diameter of tubing
$\boldsymbol{E}_\theta$ = exit age distribution of the fluid in terms of the dimensionless residence time
f = initiator efficiency
$\boldsymbol{F}$ = exit age distribution of the fluid, $\int \mathrm{E}_\theta \, \mathrm{dt}$
I = initiator concentration, mol/L; I_j^D of droplet j, I_i^P, of plug i
k_d = initiator decomposition rate constant, s^1
k_p = propagation rate constant, L $\cdot$ mol^{-1} $\cdot$ s^{-1}
k_t = termination rate constant, L $\cdot$ mol^{-1} $\cdot$ s^{-1}
L = length, cm; L_r, reactor length, L_p, plug length, L_g, gap length
n_d = number of droplets
n_p = number of plugs
P_i = plug i
q_D = volumetric flow rate of droplets, cm^3 $\cdot$ s^{-1}
Re = reynolds number, dimensionless, $d_i \, u\rho/\mu$
t = time s; t_d time to traverse one droplet length, t_g time to traverse one gap length t_p, time to traverse one plug length
u = average bulk fluid velocity, cm $\cdot$ s^{-1}
V = volume, cm^3; V_0, initial plug volume V_D, droplet volume V_i^P, volume plug i, $V_{P,1}$, volume of plug 1 cm in length at d_{iO}
X_i = Conversion, plug i

Literature Cited

1. Darling TR, Davis TP, Fryd M, Gridnev AA, Haddleton DM, Ittel SD, Matheson Jr. RR, Moad G, Rizzardo E. *J Polym Sci Part A: Polym Chem.* 2000;38:1706-1707.
2. Wang JS, Matyjaszewski K. Controlled living radical polymerization - Atom-transfer radical polymerization in the presence of transition-Metal complexes. *J Am Chem Soc.* 1995;117:5614-5615.
3. Kato M, Kamigaito M, Sawamoto M, Higashimura T. Polymerization of methyl-methacrylate with the carbon-tetrachloride dichlorotris(triphenylphosphine)ruthenium(II) methylaluminum Bis(2,6-di-tert-butylphenoxide) initiating system - Possibility of living radical polymerization. *Macromolecules.* 1995;28:1721-1723.
4. Solomon DH, Rizzardo E, Cacioli P. *Polymerization process and polymers produced thereby*. US patent 4 581 429; 1985.
5. Krstina J, Moad G, Rizzardo E, Winzor CL, Berge CT, Fryd M. Narrow polydispersity block-copolymers by free-radical polymerization in the presence of macromonomers. *Macromolecules.* 1995;28:5381-5385.
6. Moad CL, Moad G, Rizzardo E, Thang SH. Chain transfer activity of omega-unsaturated methyl methacrylate oligomers. *Macromolecules.* 1996;29:7717-7726.
7. Braslau R, O'Bryan G, Nilsen A, Henise J, Thongpaisanwong T, Murphy E, Mueller L, Ruehl J. The synthesis and evaluation of new alpha-hydrogen nitroxides for 'Living' free radical polymerization. *Synthesis-Stuttgart.* 2005:1496-1506.
8. Drockenmuller E, Lamps JP, Catala JM. Living/controlled radical polymerization of ethyl and *n*-butyl acrylates at 90 °C mediated by beta-sulfinyl nitroxides: Influence of the persistent radical stereochemistry. *Macromolecules.* 2004;37:2076-2083.
9. Moad G, Mayadunne RTA, Rizzardo E, Skidmore M, Thang SH. Synthesis of novel architectures by radical polymerization with reversible addition fragmentation chain transfer (RAFT polymerization). *Macromol Symp.* 2003;192:1-12.
10. Moad G, Chiefari, J, Chong, YK, Krstina, J, Mayadunne, RTA, Postma, A, Rizzardo, E, Thang, SH. Living free radical polymerization with reversible addition-fragmentation chain transfer (the life of RAFT). *Polym Int.* 2000;49:993-1001.
11. de Brouwer H, Tsavalas JG, Schork FJ, Monteiro MJ. Living radical polymerization in miniemulsion using reversible addition-fragmentation chain transfer. *Macromolecules.* 2000;33:9239-9246.
12. Charleux B. Theoretical aspects of controlled radical polymerization in a dispersed medium. *Macromolecules.* 2000;33:5358-5365.
13. Cunningham MF. Recent progress in nitroxide-mediated polymerizations in miniemulsion. *Cr Chim.* 2003;6:1351-1374.
14. Cunningham MF, Tortosa K, Ma JW, McAuley KB, Keoshkerian B, Georges MK. Nitroxide mediated living radical polymerization in miniemulsion. *Macromol Symp.* 2002;182:273-282.
15. Farcet C, Belleney J, Charleux B, Pirri R. Structural characterization of nitroxide-terminated poly(*n*-butyl acrylate) prepared in bulk and miniemulsion polymerizations. *Macromolecules.* 2002;35:4912-4918.
16. Simms RW, Davis TP, Cunningham MF. Xanthate-mediated living radical polymerization of vinyl acetate in miniemulsion. *Macromol Rapid Comm.* 2005;26:592-596.
17. Tortosa K, Smith JA, Cunningham MF. Synthesis of polystyrene-block-poly (butyl acrylate) copolymers using nitroxide-mediated living radical polymerization in miniemulsion. *Macromol Rapid Comm.* 2001;22:957-961.
18. Farcet C, Charleux B. Nitroxide-mediated miniemulsion polymerization of *n*-butyl acrylate: Synthesis of controlled homopolymers and gradient copolymers with styrene. *Macromol Symp.* 2002;182:249-260.
19. Farcet C, Lansalot M, Pirri R, Vairon JP, Charleux B. Polystyrene-block-poly(butyl acrylate) and polystyrene-block-poly[(butyl acrylate)-co-styrene] block copolymers prepared via controlled free-radical miniemulsion polymerization using degenerative iodine transfer. *Macromol Rapid Comm.* 2000;21:921-926.
20. Keoshkerian B, MacLeod PJ, Georges MK. Block copolymer synthesis by a miniemulsion stable free radical polymerization process. *Macromolecules.* 2001;34:3594-3599.
21. Matyaszewski K, Qiu J, Tsarevsky NV, Charleux B. Atom transfer radical polymerization of n-butyl methacrylate in an aqueous dispersed system: A miniemulsion approach. *J Polym Sci Part A: Polym Chem.* 2000;38:4724-4734.
22. Li C, Min K, Matyjaszewski K. ATRP in Waterborne Miniemulsion via a Simultaneous Reverse and Normal Initiation Process. 2004.
23. Li M, Matyjaszewski K. Further progress in atom transfer radical polymerizations conducted in a waterborne system. *J Polym Sci Part A: Polym Chem.* 2003;41:3606-3614.

24. Li M, Matyjaszewski K. Reverse atom transfer radical polymerization in miniemulsion. *Macromolecules.* 2003;36:6028-6035.
25. Ma JW, Cunningham MF, McAuley KB, Keoshkerian B, Georges M. Nitroxide mediated living radical polymerization of styrene in miniemulsion - modelling persulfate-initiated systems. *Chem Eng Sci.* 2003;58:1177-1190.
26. Ma JW, Cunningham MF, McAuley KB, Keoshkerian B, Georges MK. Model studies of nitroxide-mediated styrene miniemulsion polymerization - Opportunities for process improvement. *Macromol Theor Simul.* 2003;12:72-85.
27. Ma JW, Smith JA, McAuley KB, Cunningham MF, Keoshkerian B, Georges MK. Nitroxide-mediated radical polymerization of styrene in miniemulsion: model studies of alkoxyamine-initiated systems. *Chem Eng Sci.* 2003;58:1163-1176.
28. Butte A, Storti G, Morbidelli M. Miniemulsion living free radical polymerization by RAFT. *Macromolecules.* 2001;34:5885-5896.
29. Luo YW, Tsavalas J, Schork FJ. Theoretical aspects of particle swelling in living free radical miniemulsion polymerization. *Macromolecules.* 2001;34:5501-5507.
30. Tsavalas JG, Schork FJ, de Brouwer H, Monteiro MJ. Living radical polymerization by reversible addition-fragmentation chain transfer in ionically stabilized miniemulsions. *Macromolecules.* 2001;34:3938-3946.
31. Prescott SW, Ballard MJ, Rizzardo E, Gilbert RG. Successful use of RAFT techniques in seeded emulsion polymerization of styrene: Living character, RAFT agent transport, and rate of polymerization. *Macromolecules.* 2002;35:5417-5425.
32. Cunningham MF, Xie M, McAuley KB, Keoshkerian B, Georges MK. Nitroxide-mediated styrene miniemulsion polymerization. *Macromolecules.* 2002;35:59-66.
33. Lansalot M, Davis TP, Heuts JPA. RAFT miniemulsion polymerization: Influence of the structure of the RAFT agent. *Macromolecules.* 2002;35:7582-7591.
34. Luo YW, Liu X. Reversible addition-fragmentation transfer (RAFT) copolymerization of methyl methacrylate and styrene in miniemulsion. *J Polym Sci Part A: Polym Chem.* 2004;42:6248-6258.
35. Mcleary JB, Tonge MP, Roos DD, Sanderson RD, Klumperman B. Controlled, radical reversible addition-fragmentation chain-transfer polymerization in high-surfactant concentration ionic miniemulsions. *J Polym Sci Part A: Polym Chem.* 2004;42:960-974.
36. MacLeod PJ, Barber R, Odell PG, Keoshkerian B, Georges MK. Stable free radical miniemulsion polymerization. *Macromol Symp.* 2000;155:31-38.
37. Russum JP, Barbre ND, Jones CW, Schork FJ. Miniemulsion reversible addition fragmentation chain transfer polymerization of vinyl acetate. *J Polym Sci Part A: Polym Chem.* 2005;43:2188-2193.
38. Russum JP, Jones CW, Schork FJ. Continuous reversible addition-fragmentation chain transfer polymerization in miniemulsion utilizing a multi-tube reaction system. *Macromol Rapid Comm.* 2004;25:1064-1068.
39. Smulders WW, Jones CW, Schork FJ. Synthesis of block copolymers using RAFT miniemulsion polymerization in a train of CSTRs. *Macromolecules.* 2004;37:9345-9354.
40. Russum JP, Jones CW, Schork FJ. Continuous living polymerization in miniemulsion using reversible addition fragmentation chain transfer (RAFT) in a tubular reactor. *Ind Eng Chem Res.* 2005;44:2484-2493.
41. Smulders WW, Jones CW, Schork FJ. Continuous RAFT miniemulsion polymerization of styrene in a train of CSTRs. *AIChE J.* 2005;51:1009-1021.
42. Enright TE, Cunningham MF, Keoshkerian B. Nitroxide-mediated polymerization of styrene in a continuous tubular reactor. *Macromol Rapid Comm.* 2005;26:221-225.
43. Shen YQ, Zhu SP. Continuous atom transfer radical block copolymerization of methacrylates. *AIChE J.* 2002;48:2609-2619.
44. Shen YQ, Zhu SP, Pelton R. Packed column reactor for continuous atom transfer radical polymerization: Methyl methacrylate polymerization using silica gel supported catalyst. *Macromol Rapid Comm.* 2000;21:956-959.
45. Quinn JF, Rizzardo E, Davis TP. Ambient temperature reversible addition-fragmentation chain transfer polymerisation. *Chem Commun.* 2001:1044-1045.
46. Levenspiel O. *Chemical reaction engineering*. 3rd ed. New York, NY: Wiley; 1999.
47. Hutchinson M, De Hoog F. Smoothing noisy data with spline functions. *Numer Math.* 1985;47:99-106.
48. van der Laan ET. Notes on the diffusion-type model for the longitudinal mixing in flow. *Chem Eng Sci.* 1958;7:187-191.
49. Shoaf GL, Poehlein GW. Batch and Continuous Emulsion Copolymerization of Ethyl Acrylate and Methacrylic-Acid. *Polym-Plast Technol.* 1989;28:289-317.
50. Lee HC, Poehlein GW. Continuous Tube-CSTR Reactor System for Emulsion Polymerization Kinetic-Studies. *Chem Eng Sci.* 1986;41:1023-1030.

Manuscript received Aug. 25, 2005, and revision received Oct. 14, 2005.